PHYSICAL REVIEW B **80**, 060502(R) (2009)

Evidence for two-gap nodeless superconductivity in $SmFeAsO_{1-x}F_x$ from point-contact Andreev-reflection spectroscopy

D. Daghero,[1] M. Tortello,[1] R. S. Gonnelli,[1] V. A. Stepanov,[2] N. D. Zhigadlo,[3] and J. Karpinski[3]
[1]*Dipartimento di Fisica and CNISM, Politecnico di Torino, 10129 Torino, Italy*
[2]*P.N. Lebedev Physical Institute, Russian Academy of Sciences, 119991 Moscow, Russia*
[3]*Laboratory for Solid State Physics, ETHZ, CH-8093 Zurich, Switzerland*
(Received 23 June 2009; published 5 August 2009)

Point-contact Andreev-reflection spectroscopy measurements were performed in $SmFeAsO_{1-x}F_x$ polycrystals with $x=0.09$ ($T_c \simeq 42$ K) and $x=0.20$ ($T_c \simeq 52$ K). In all cases the experimental conductance curves reproducibly exhibit low-energy peaks and higher-energy shoulders (at 4–6 and 16–20 meV, respectively, for $x=0.20$), which indicate the presence of two nodeless superconducting gaps. While the single-band Blonder-Tinkham-Klapwijk model can only reproduce a small central portion of a given conductance curve, the two-gap one accounts remarkably well for the shape of the whole experimental dI/dV vs V curve. The fit of the normalized curves gives $\Delta_1(0)=6.15\pm0.45$ meV and $\Delta_2(0)=18\pm3$ meV for $x=0.20$, while for $x=0.09$ the values $\Delta_1(0)=4.9\pm0.5$ meV and $\Delta_2(0)=15\pm1$ meV are obtained. In all cases, both gaps close at the same temperature and follow a BCS-like behavior.

DOI: 10.1103/PhysRevB.80.060502 PACS number(s): 74.50.+r, 74.45.+c, 74.70.Dd

The experimental evidence of superconductivity in F-doped LaFeAsO (Ref. 1) paved the way to the discovery of a new class of superconductors that, with the exception of copper-based high-T_c superconductors, show the highest critical temperatures known so far, with the record $T_c=55$ K in F-doped or oxygen-deficient SmFeAsO.[2,3]

SmFeAsO is semimetallic and shows a spin-density-wave (SDW) antiferromagnetic order as well as a tetragonal-to-orthorombic structural transition at ~ 140 K.[4] Charge doping in the FeAs planes (obtained, for example, by partial substitution of oxygen with fluorine) rapidly suppresses the SDW order until superconductivity sets in.[4] The vicinity of the superconducting state to a magnetic one raises many questions concerning the pairing mechanism that is responsible for superconductivity. Local-density approximation calculations for the LaFeAsOF system[5] (performed by assuming a nonmagnetic ground state) showed that the electron-phonon coupling is not sufficient to explain the observed T_c. An extended $s\pm$-wave pairing with a sign reversal of the order parameter between different sheets of the Fermi surface was thus proposed[6] and shown to be compatible with a coupling mechanism related to spin fluctuations, as well as with a multigap scenario.[7,8] On the experimental side, growing evidence for multigap superconductivity in Fe-As-based compounds is being provided by several experimental works.[9–17]

A general consensus on the pairing mechanism in these new superconductors, and especially on the number, nature, and symmetry of the superconducting order parameter(s) is however still to be achieved. For example, point-contact Andreev-reflection spectroscopy (PCAR) is one of the most powerful techniques to determine the gap value(s) and its (their) symmetry, but the results of PCAR studies performed so far in $SmFeAsO_{1-x}F_x$ (Refs. 17 and 18) appear in complete disagreement. Chen *et al.*[18] observed a single BCS-like *s*-wave gap, while Wang *et al.*[17] reported two nodal order parameters.

In this Rapid Communication, we report the results of PCAR measurements in state-of-the-art polycrystalline samples of $SmFeAsO_{1-x}F_x$. The experimental data for $x=0.20$ reproducibly show the presence of two nodeless energy gaps, $\Delta_1(0)=6.15\pm0.45$ meV and $\Delta_2(0)=18\pm3$ meV, both approximately showing a BCS-like temperature dependence and closing at the same temperature T_c^A, which is the critical temperature of the junction. In all the point contacts we made on $SmFeAsO_{0.8}F_{0.2}$, T_c^A is always close to the bulk T_c. In samples with $x=0.09$ a reduction of 25% in T_c^A with respect to optimal doping corresponds to a reduction of about 20% in $\Delta_1(0)$ and $\Delta_2(0)$.

The polycrystalline samples of $SmFeAsO_{1-x}F_x$ were synthesized under high pressure starting from SmAs, FeAs, SmF_3, Fe_2O_3, and Fe. After the materials were pulverized and sealed in a BN crucible, a pressure of 30 kbar was applied at room temperature. The temperature was then increased up to 1350–1450 °C in 1 h, kept for 4.5 h at this value, and then fast decreased down to room temperature. Finally the pressure was released.[19] The resulting samples are very compact and made up of shiny crystallites whose size, as revealed by scanning electron microscopy images, is on the order of 30 μm. The bulk critical temperature, defined here at the onset of the superconducting transition measured by dc magnetization, is $T_c=52$ K for $x=0.20$ (inset to Fig. 1) and $T_c=42$ K for $x=0.09$.

The point contacts were made by putting a small drop ($\varnothing \leq 50$ μm) of Ag conducting paste on the fresh surface of the sample instead of pressing a metallic tip against it as in the standard PCAR technique. This pressureless technique was already successfully used in MgB_2, CaC_6, ruthenocuprates, A15, and so on.[20,21] The contacts made in this way are likely to be the parallel of some nanojunctions established between the Ag grains (2–10 μm in size) and the $SmFeAsO_{1-x}F_x$ crystallites ($\simeq 30$ μm) and are very stable under thermal cycling. This allowed us to easily record the conductance curves up to 200 K.

When performing PCAR experiments, one should check that the contact is ballistic, i.e., that its radius a is smaller than the electronic mean free path, ℓ, in the superconductor.[22] In these conditions, injected charges do not lose energy in the contact region and energy-resolved spec-

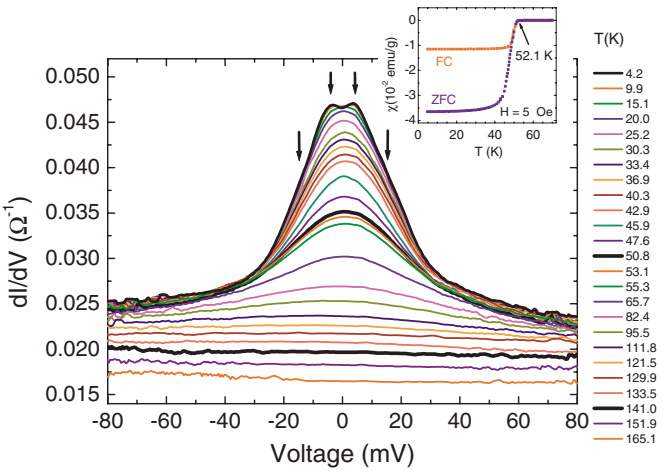

FIG. 1. (Color online) Temperature dependence of the raw conductance curves of a point contact with $T_c^A \sim 51$ K on $SmFeAsO_{0.8}F_{0.2}$. The curve at 4.2 K (top thick line) features two peaks and two shoulders (arrows). The curve at T_c^A (middle thick line) has a humplike shape, which flattens at ~140 K (bottom thick line). The inset shows the dc susceptibility of the sample.

troscopy is possible. In our case, the occurrence of multiple contacts and the poor knowledge of ℓ make this check impossible. However, the absence of heating effects in our junctions can be deduced from the general shape of the conductance curves, from the amplitude of the Andreev-reflection features, and from the absence of dips.[23]

The differential conductance dI/dV of our point contacts was obtained by taking the numerical derivative of the I-V characteristics. Figure 1 shows the raw conductance curves, measured from 4.2 up to about 165 K of a contact on $SmFeAsO_{0.8}F_{0.2}$ whose normal-state resistance is 40 Ω. The critical temperature of the junction ($T_c^A = 51 \pm 1$ K) is reached when the conductance at zero bias decreases abruptly (due to the collapse of the gaps) *and* the subsequent curves, although equally spaced in temperature, look almost superimposed to one another. The lowest-temperature curve (top thick line) shows clear Andreev-reflection features such as two peaks at about ±4 mV, certainly related to a superconducting gap,[18] plus two broad shoulders at higher bias that, as in MgB_2,[20] can indicate a second larger gap. In all our contacts on this sample the normal-state conductance measured at T_c^A (middle thick line in Fig. 1) features a hump at zero bias that gradually decreases upon heating until it completely disappears (bottom thick line) around the Néel temperature of the parent compound, $T_N \sim 140$ K.[4] This might suggest a magnetic origin of this hump even though this point deserves further investigation. A similar downward curvature of the normal-state spectrum was also found in recent PCAR (Ref. 11) and angle resolved photoemission spectroscopy[10] measurements in $Ba_{0.6}K_{0.4}Fe_2As_2$. Finally, the conductance is always asymmetric for positive/negative bias at all temperatures, even above T_c^A and even when the zero-bias hump disappears. This asymmetry was also observed in other PCAR measurements.[11,12,18]

In view of a comparison with a theoretical model, the experimental conductance curves (dI/dV vs V) of each junction had to be normalized, i.e., divided by the relevant

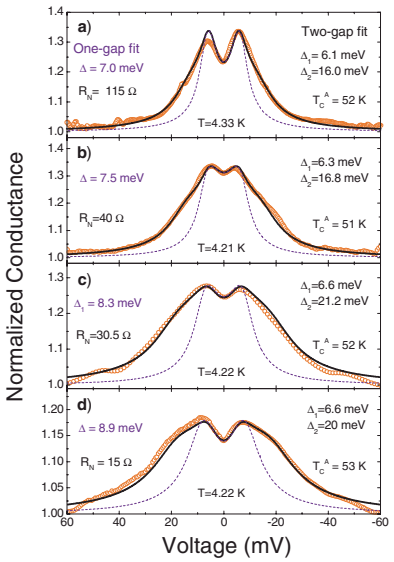

FIG. 2. (Color online) (a)–(d) Normalized conductance curves (symbols) at 4.2 K in $SmFeAsO_{0.8}F_{0.2}$. The contact resistance, R_N, decreases from top to bottom. The curves are reported together with their relevant one-gap (dash lines) and two-gap (solid lines) BTK fits. The gap values are indicated on the left (single-gap fit) and on the right (two-gap fit).

normal-state conductance. Since the upper critical field is very high,[24] the normal-state conductance at $T < T_c^A$ is not experimentally accessible. The normalization was therefore performed by using the normal-state conductance curve measured at T_c^A.

Figure 2 shows several examples of low-temperature normalized conductance curves (symbols) obtained in an optimally doped sample ($x=0.20$). In most cases, the amplitude of the Andreev signal is on the order of 20–30 % (similar to what observed in Refs. 18, 20, and 21). In other PCAR measurements in Fe-based superconductors the emergence of zero-bias conductance peaks (ZBCPs) was observed,[18,25] depending on the contact resistance and thus on the pressure applied by the tip. This problem is completely overcome in our case, where no pressure is applied to the sample. The systematic absence of ZBCP in our curves completely rules out the d-wave symmetry for the gaps. As a matter of fact, all the Andreev-reflection curves calculated within the generalized Blonder-Tinkham-Klapwijk (BTK) model in the d-wave case[26] and by using parameters similar to the experimental ones, feature clear ZBCP at 4.2 K whenever the current is injected at an angle $\beta > 15°$ with respect to the antinodal direction.[27] Even if one averages over all possible injection angles from 0 to $\pi/4$ to account for the polycrystalline nature of the sample and the multiple contacts, a clear ZBCP is always present in the theoretical curves and should thus be detected experimentally.

The normalized conductance curves were then fitted with a s-wave two-band BTK model[28] generalized to include broadening effects[29] and the angular dependence of the charge injection probability.[26] In this model,[30] the normalized conductance is the weighted sum of the conductances of the two bands, $G = w_1 G_1^{BTK} + (1-w_1) G_2^{BTK}$ where w_1 is the weight of band 1. Each conductance depends on three pa-

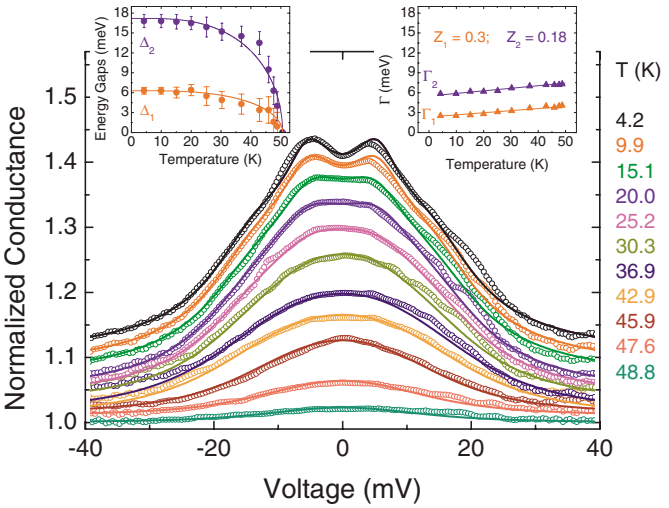

FIG. 3. (Color online) Temperature dependence of the normalized conductance curve of Fig. 2(b) (symbols) together with the two-gap BTK fits of the negative-bias side (lines). The curves are vertically shifted for clarity. The raw data are those shown in Fig. 1, and the insets show the temperature dependence of Δ_1 and Δ_2 and of Γ_1 and Γ_2, respectively.

rameters: the gap Δ, a broadening parameter Γ,[29] and the effective potential barrier parameter Z.[26,28] The model contains seven fitting parameters (three for each band plus w_1), which are not totally free in the sense that, if one fits the whole temperature dependence of a conductance curve, Z_1 and Z_2, the weight w_1 and the broadening parameters Γ_1 and Γ_2 should remain approximately constant.

In Fig. 2, the normalized experimental curves are compared to the relevant two-gap fitting curves (solid lines) and to the single-gap ones (dash lines). Clearly, the single-gap model can only account for a small portion of the spectra (as in Ref. 18). The relevant gap values range from 7.0 to 8.9 meV, corresponding to $2\Delta(0)/k_BT_c^A=3.1-3.9$. The two-gap fit can instead reproduce the experimental curves remarkably better and gives $\Delta_1=6.1-6.6$ meV and $\Delta_2=16-21$ meV. Thanks to the amplitude of the Andreev signal, the ratio $\Gamma_i(0)/\Delta_i(0)$ is usually $\sim 0.4-0.6$ or smaller; w_1 is 0.55 ± 0.10 depending on the junction. The normalized conductances often show a residual right/left asymmetry, which mainly affects the determination of Δ_2; this asymmetry might be due to the unconventional shape of the background, which is itself asymmetric and changes with temperature. A fit of the positive- and negative-bias sides of the normalized curves was carried out to evaluate the uncertainty on Δ_2 arising from this asymmetry.

An example of how the two-band model can fit the normalized conductance curves recorded at different temperatures is given in Fig. 3. Here, the experimental curves (symbols) are slightly offset for clarity and compared to the BTK curves (lines) that best fit their negative-bias side. The parameters Z_1 and Z_2 used for the fit are indicated in the labels of the right inset; a small decrease (on the order of 20% of these values) had to be allowed to obtain a good fit of the whole temperature dependence—but this might simply mean that the normal-state conductance has a sharper peak at low

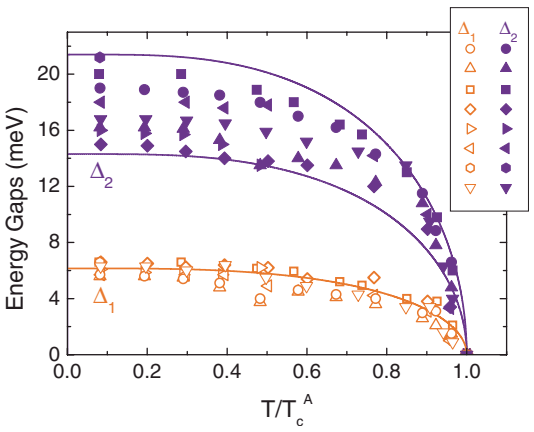

FIG. 4. (Color online) Temperature dependence of the gaps Δ_1 (open symbols) and Δ_2 (solid symbols) in $SmFeAsO_{0.80}F_{0.2}$ as extracted from the two-gap fit of various conductance curves. Lines are BCS-like curves. Details are in the text.

temperature than at T_c^A. The values of the gaps Δ_1 and Δ_2 and of the broadening parameters Γ_1 and Γ_2 are reported in the insets. Note that the temperature dependence of the gaps is compatible with a BCS-like trend, with gap ratios $2\Delta_1(0)/k_BT_c^A=2.87$ and $2\Delta_2(0)/k_BT_c^A=7.66$.

The temperature dependence of the gaps in $SmFeAsO_{0.8}F_{0.2}$ obtained from the two-gap BTK fit of the curves shown in Fig. 3 and of various other curves is reported in Fig. 4. The reproducibility of the small gap (open symbols) is noticeable: Δ_1 is close to 6 meV at low temperature and follows a BCS-like trend up to T_c^A, which is always between 50 and 53 K in our contacts (the normalized temperature T/T_c^A is used in Fig. 4 for homogeneity). As far as Δ_2 is concerned, its behavior *in each set of data* is compatible with a BCS-like trend, but the spread of values between different data sets is rather wide: all the data fall in a region

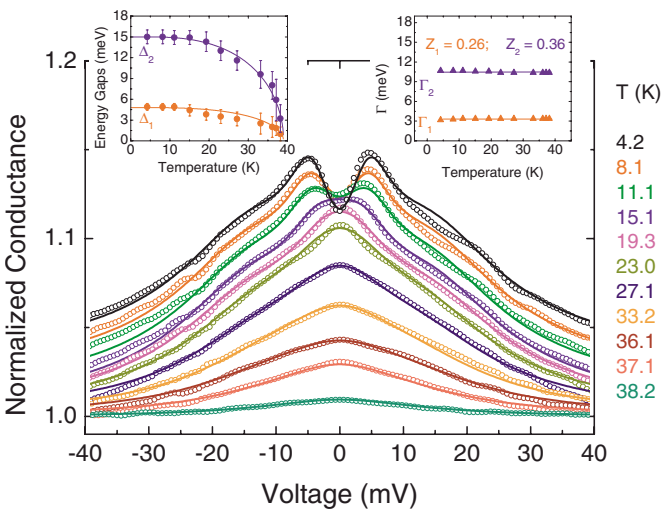

FIG. 5. (Color online) Temperature dependence of the normalized conductance curves (symbols) and of the two-gap BTK fits of their negative-bias side (lines) in a point contact on $SmFeAsO_{0.91}F_{0.09}$. The curves are vertically shifted for clarity. The insets show the temperature dependence of Δ_1 and Δ_2 and of Γ_1 and Γ_2, respectively.

bounded by two BCS-like curves with gap ratios $2\Delta_2(0)/k_BT_c^A \simeq 7$ and 9, respectively. Incidentally, this region is centered on a value $\Delta_2 \simeq 18$ meV that is close to that determined with infrared ellipsometry.[31] The spread of Δ_2 values shown in Fig. 4 is not an artifact due to our particular PCAR technique since in MgB_2, for example, both the gaps were determined in the same way with great accuracy (± 0.5 meV at most, at 4.2 K).

At low temperature, the ratio of the gaps Δ_2/Δ_1 is about 3, as also observed in other pnictides.[11–13] Such a high value can be obtained within the Eliashberg theory provided that the simplest interband-only $s\pm$-wave model[6] is extended to the case of three energy bands with a strong interband coupling between two of them and a small boson frequency.[32]

Figure 5 shows the temperature dependence of the normalized conductance curves (symbols) and the relevant two-gap fits (lines) for an underdoped $SmFeAsO_{1-x}F_x$ sample with $x=0.09$. As in the previous cases, the raw conductance curves were divided by the normal-state conductance measured at T_c^A. Unlike in the $x=0.20$ samples, this curve did not show the "hump" at zero bias but a smooth positive curvature superimposed to the usual right/left asymmetry. This shape did not change significantly upon increasing the temperature up to 180 K. Looking at our experimental data on various samples, we found indeed that the percentage of contacts with zero-bias hump in the normal-state conductance decreases upon decreasing the doping content. Whenever the hump is present at T_c^A, it disappears around 140 K so that the conductance curves flatten (as in Fig. 1); otherwise, the shape of the conductance curves changes much less on heating. This interesting behavior deserves further investigation and will be the subject of a forthcoming paper.

In Fig. 5 the left and right insets show the temperature dependence of the gaps and of the Γ parameters obtained from the fit of the negative-bias side of the conductance curves. In strong analogy with the results obtained in optimally doped samples, the shape of the experimental curves and the goodness of the two-band BTK fit strongly suggest the presence of two gaps $\Delta_1(0)=4.9\pm0.5$ meV and $\Delta_2(0)=15\pm1$ meV, reduced by about 20% with respect to optimal doping. The temperature dependence of these gaps up to $T_c^A=39$ K is again compatible with a BCS-like behavior. The gap ratios are $2\Delta_1(0)/k_BT_c^A=2.92$ and $2\Delta_2(0)/k_BT_c^A=8.94$, similar to the highest observed in optimally doped samples. Interestingly, the ratio of the gaps $\Delta_2(0)/\Delta_1(0)\simeq 3$ is the same as in optimally doped samples ($x=0.20$).

In summary, we performed pressureless PCAR measurements in $SmFeAsO_{1-x}F_x$ polycrystals with $x=0.20$ and 0.09. The experimental low-temperature conductance curves show peaks at low bias and shoulders at higher voltage, which can be interpreted as being due to two nodeless superconducting gaps. Indeed, the two-gap BTK model accounts remarkably well for the whole shape of the normalized curves, apart from their asymmetry. Upon increasing the temperature, the two gaps approximately follow a BCS-like temperature dependence and close at the same temperature, T_c^A. In optimally doped samples ($x=0.20$) the reproducibility of the small gap Δ_1 over different contacts is rather good, while the spread of Δ_2 is very large, possibly because of the uncertainty in the normalization and the asymmetry of the PCAR spectra. On average, we obtained $\Delta_1(0)=6.15\pm0.45$ meV and $\Delta_2(0)=18\pm3$ meV with ratios $2\Delta_1(0)/k_BT_c^A=2.5-3$ and $2\Delta_2(0)/k_BT_c^A=7-9$, respectively. These results are basically confirmed in underdoped samples ($x=0.09$) with $T_c^A\simeq 39$ K, where we obtained $\Delta_1(0)=4.9\pm0.5$ meV and $\Delta_2(0)=15\pm1$ meV and similar high gap ratios that, as recently shown, *can* be reproduced theoretically.[32] All these results, together with other experimental findings in pnictide superconductors,[9–17] point toward a common multigap scenario to most (if not all) Fe-As-based superconductors.

We thank G. A. Ummarino, I. I. Mazin, P. Szabó, L. F. Cohen, and Y. Fasano for useful discussions. V.A.S. acknowledges support by the Russian Foundation for Basic Research (Project No. 09-02-00205). The work at ETH was supported by MaNEP program and the work in Torino by the PRIN Project No. 2006021741.

[1] Y. Kamihara *et al.*, J. Am. Chem. Soc. **130**, 3296 (2008).
[2] Z. A. Ren *et al.*, Chin. Phys. Lett. **25**, 2215 (2008).
[3] Z. A. Ren *et al.*, EPL **83**, 17002 (2008).
[4] A. J. Drew *et al.*, Nature Mater. **8**, 310 (2009).
[5] L. Boeri *et al.*, Phys. Rev. Lett. **101**, 026403 (2008).
[6] I. I. Mazin *et al.*,Phys. Rev. Lett. **101**, 057003 (2008).
[7] L. Benfatto *et al.*, Phys. Rev. B **78**, 140502(R) (2008).
[8] I. I. Mazin and J. Schmalian, Physica C **469**, 614 (2009).
[9] F. Hunte *et al.*, Nature (London) **453**, 903 (2008).
[10] H. Ding *et al.*, EPL **83**, 47001 (2008).
[11] P. Szabó *et al.*, Phys. Rev. B **79**, 012503 (2009).
[12] R. S. Gonnelli *et al.*, Phys. Rev. B **79**, 184526 (2009).
[13] S. Kawasaki *et al.*, Phys. Rev. B **78**, 220506(R) (2008).
[14] K. Matano *et al.*, EPL **83**, 57001 (2008).
[15] P. Samuely *et al.*, Supercond. Sci. Technol. **22**, 014003 (2009).
[16] M. Pan *et al.*, arXiv:0808.0895 (unpublished).
[17] Y. Wang *et al.*, Supercond. Sci. Technol. **22**, 015018 (2009).
[18] T. Y. Chen *et al.*, Nature (London) **453**, 1224 (2008).
[19] N. D. Zhigadlo *et al.*, J. Phys.: Condens. Matter **20**, 342202 (2008).
[20] R. S. Gonnelli *et al.*, Phys. Rev. Lett. **89**, 247004 (2002).
[21] R. S. Gonnelli *et al.*, Phys. Rev. Lett. **100**, 207004 (2008).
[22] A. M. Duif *et al.*, J. Phys.: Condens. Matter **1**, 3157 (1989).
[23] G. Sheet *et al.*, Phys. Rev. B **69**, 134507 (2004).
[24] C. Senatore *et al.*, Phys. Rev. B **78**, 054514 (2008).
[25] K. A. Yates *et al.*, Supercond. Sci. Technol. **21**, 092003 (2008).
[26] S. Kashiwaya *et al.*, Phys. Rev. B **53**, 2667 (1996).
[27] N. Stefanakis, J. Phys.: Condens. Matter **13**, 1265 (2001).
[28] G. E. Blonder *et al.*, Phys. Rev. B **25**, 4515 (1982).
[29] A. Plecenik *et al.*, Phys. Rev. B **49**, 10016 (1994).
[30] Recently, some new models for Andreev reflection at the interface with a $s\pm$ superconductor have been proposed. They predict interference effects that, for *low-transparency* barriers and at $T\rightarrow 0$ (which is not our case), make the conductance curves show peaks that depend on the direction of current injection, which is out of control in a polycrystal.
[31] A. Dubroka *et al.*, Phys. Rev. Lett. **101**, 097011 (2008).
[32] G. Ummarino *et al.*, arXiv:0904.1808 (unpublished).